Fluorescent Molecular Probe for *In Vivo* Targeting and Live Cell Imaging of Intracellular Pathogenic *E. coli*

Shailendra Koirala[a], Yalini H. Wijesundara[a], Dong-Hao Li[d], Jashkaran Gadhvi[c], Ryanne N. Ehrman[a], Samuel Cornelius[c], Miguel A. Gaspar[a], Thien-Quang N. Nguyen[a], Orikeda Trashi[a], Ikeda Trashi[a], Sneha Kumari[a], Laurel M. Hagge[a], Thomas S. Howlett[a], Bradley D. Smith[d], Nicole J. De Nisco[c*], and Jeremiah J. Gassensmith[a,b*]

[a] Department of Chemistry and Biochemistry
The University of Texas at Dallas
800 West Campbell Road, Richardson, Texas 75080-3021, United States
[b] Department of Biomedical Engineering
The University of Texas at Dallas
800 West Campbell Road, Richardson, Texas 75080-3021, United States
[c] Department of Biological Sciences
The University of Texas at Dallas
800 West Campbell Road, Richardson, Texas 75080-3021, United States
[d] Department of Chemistry and Biochemistry
University of Notre Dame
236 Nieuwland Science Hall, Notre Dame, Indiana 46556, United States

Email: nicole.denisco@utdallas.edu and gassensmith@utdallas.edu

Abstract

Intracellular bacterial infections are difficult to diagnose and treat because the host cells shelter the bacteria from molecular recognition by imaging agents, antibiotics, and the immune system. This problem arises when bladder epithelial cells are infected by uropathogenic *Escherichia coli* (UPEC)—one of the causative agents of urinary tract infection (UTI). UTIs are among the most common bacterial infections and a worldwide health concern. It is challenging to design molecular probes for intracellular UPEC imaging or targeted antibiotic treatment because the probe must possess multiple capabilities—it must permeate the host cell plasma membrane and selectively associate with the intracellular UPEC. Here, we report a “first-in-class” fluorescent probe called BactVue that is comprised of two structural components: a modified zinc (II)-2,2’-dipicolylamine complex (Zn-Oxy-DPA) as the bacteria targeting unit and an appended near-infrared cyanine fluorophore that is hydrophilic but with near-neutral electrostatic charge. The unique capacity of BactVue to target intracellular UPEC was demonstrated by a series of *in vitro* and *in vivo* fluorescence imaging studies. The results show that BactVue can penetrate infected human bladder epithelial cells and stain intracellular UPEC both *in vitro* and in a mouse model of UTI. These results support the feasibility of incorporating BactVue into diagnostic near-infrared fluorescence imaging methods that visualize the location of infected bladder cells during active UTI. There is also great potential to develop homologous molecular probes for other imaging modalities and to design new therapeutic approaches that exploit selective targeting by the Zn-Oxy-DPA unit.

https://doi.org/10.26434/chemrxiv-2024-h3p4f **ORCID:** https://orcid.org/0000-0001-6400-8106 Content not peer-reviewed by ChemRxiv. **License:** CC BY-NC-ND 4.0

Introduction

Urinary tract infection (UTI) is a common bacterial infection worldwide that can lead to hospitalization in severe cases.[1-5] Women have a 50-60% lifetime occurrence rate of UTI, with 27% of those patients experiencing recurrent episodes. Research has identified uropathogenic *E. coli* (UPEC) as the primary cause of UTIs.[6, 7] The ability of UPEC to invade luminal epithelial cells of the bladder (urothelial cells) and avoid inactivation by antibiotics or the host immune system is a critical factor in establishing a persistent infection.[8-10] Recent work has shown that the bacteria invade deep bladder tissues and form intracellular bacterial communities (IBCs) in mice and humans.[4, 11, 12] These IBCs act as reservoirs that may contribute to frequent recurrence following antibiotic treatment and remission of symptoms.[8, 13] Detection of latent intracellular bacteria in a living subject is difficult; consequently, many persistent infections go undiagnosed.[14] Urine culture is commonly used to confirm a UTI; however, this method is relatively slow and resource-intensive, limiting clinical effectiveness as it cannot detect tissue-resident bacteria.[15-18] Faster diagnostic methods, such as urinary dipstick and urine microscopy, have limited diagnostic accuracy and cannot detect intracellular bacteria either.[19-21] Although IBCs are well described, unambiguous identification within living tissue is challenging and remains a major hurdle to clinical translation as—to the best of our knowledge—there are no systems capable of selectively staining live bacteria within a living cell.

The host cell plasma membrane of a living cell is a formidable barrier that protects intracellular bacterial infections such as UTIs, and there is a need for new molecular targeting strategies that enable UTI imaging and treatment.[5, 22-24] In principle, the ideal molecule for selective targeting of intracellular UPEC should possess two distinct capabilities—reversibly permeate the cell plasma membrane and selectively associate with the intracellular UPEC. Literature reports of molecules that target intracellular bacteria are rare and focus primarily on antibiotic drug conjugates.[25-28]

https://doi.org/10.26434/chemrxiv-2024-h3p4f **ORCID:** https://orcid.org/0000-0001-6400-8106 Content not peer-reviewed by ChemRxiv. **License:** CC BY-NC-ND 4.0

While large molecules such as antibodies may have attractive molecular recognition properties, their use is likely to be limited by poor membrane permeability. On the other hand, small targeting molecules might exhibit better membrane permeability, but it is challenging to design them with the appropriate cell recognition properties. In this regard, a differentiating feature between healthy mammalian cells and bacteria is the cell surface charge. The surrounding envelope of virtually all bacteria, including UPEC, has an anionic electrostatic surface, whereas the exterior electrostatic surface of healthy mammalian cell membranes is closer to neutral.[29-31] This difference in surface charge has been exploited by designing cationic molecular probes that have selective affinity for anionic bacteria membranes. The structural scope includes peptides, synthetic organic molecules, and metal coordination complexes.[32-34] Particularly effective are zinc(II) 2,2'-dipicolylamine (ZnDPA) coordination complexes, which are known to selectively target bacterial cells in complex environments, including living subjects.[29, 35, 36] The selective targeting is attributed to a synergistic combination of electrostatic attraction and zinc coordination with the abundant anionic phosphate and carboxylate groups on the polar amphiphiles in the bacterial cell wall. In addition to bacteria, ZnDPA complexes are known to target other types of cells with anionic surfaces, including dead and dying mammalian cells, though this ligand has never been shown to pass a lipid bilayer. In contrast, the modified version of the ZnDPA scaffold has a bridging oxygen atom between the two zinc(II) atoms (Zn-Oxy-DPA), which is significantly less studied, is a more compact ligand, with the Zn binding to the bridging oxygen. We suspect this ligand is more likely to interact with the cellular membrane than the more ubiquitously used ZnDPA.[37-39]

A key design element is the appended fluorescent dye.[40-43] Near-infrared (NIR) fluorescent dyes are logical choices for *in vivo* imaging owing to the relatively deep tissue penetration of long wavelength light, with minimal background autofluorescence and reduced light scattering by tissue components. [44-49] Heptamethine cyanine (Cy7) dyes possess exceptional NIR fluorescent characteristics; however, because they are naturally hydrophobic, their structures must be

https://doi.org/10.26434/chemrxiv-2024-h3p4f **ORCID:** https://orcid.org/0000-0001-6400-8106 Content not peer-reviewed by ChemRxiv. **License:** CC BY-NC-ND 4.0

modified with charged functional groups to make them water-soluble. This modification is necessary to prevent undesired processes, such as self-aggregation and non-specific binding to biological surfaces that are not the intended targets.[48, 50]{Adams, 2020 #122} Since our design goal was a molecular probe that permeated mammalian cells and reached the cytosol, there needed to be a judicious balance of molecular charge and hydrophobicity.[51] This led us to design an NIR fluorescent probe called BactVue (**Scheme 1**). The molecular structure comprises a Zn-Oxy-DPA targeting unit appended to Cy7 dye with a charge-balanced structure and two short shielding arms.[52-54] We have assessed the capacity of BactVue to target UPEC by conducting a series of *in vitro* and *in vivo* fluorescence imaging studies. We found that BactVue can penetrate infected human bladder cells and stain intracellular UPEC and can be used to visualize UPEC infection within the bladder of a living mouse model of UTI.

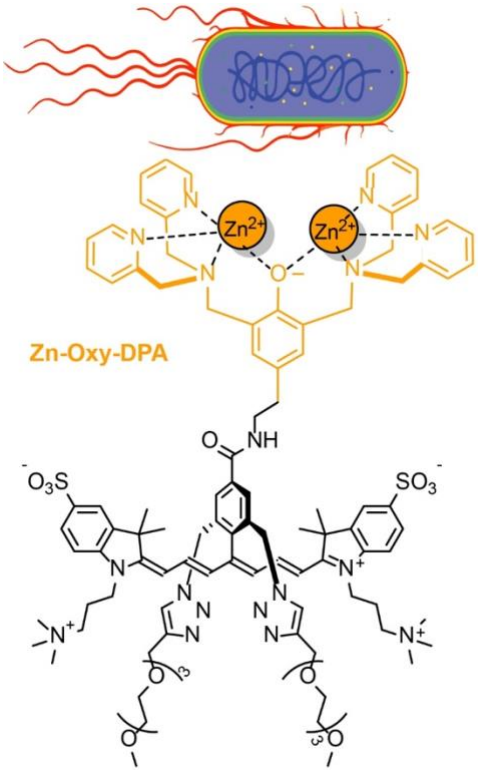

Scheme 1: Structure of BactVue. The Zn-Oxy-DPA complex (orange) is attached to a NIR fluorescent Cy7 dye that has a charge-balanced structure with two shielding arms.

https://doi.org/10.26434/chemrxiv-2024-h3p4f **ORCID:** https://orcid.org/0000-0001-6400-8106 Content not peer-reviewed by ChemRxiv. **License:** CC BY-NC-ND 4.0

Results and Discussion

In vitro staining of UTI89 bacteria

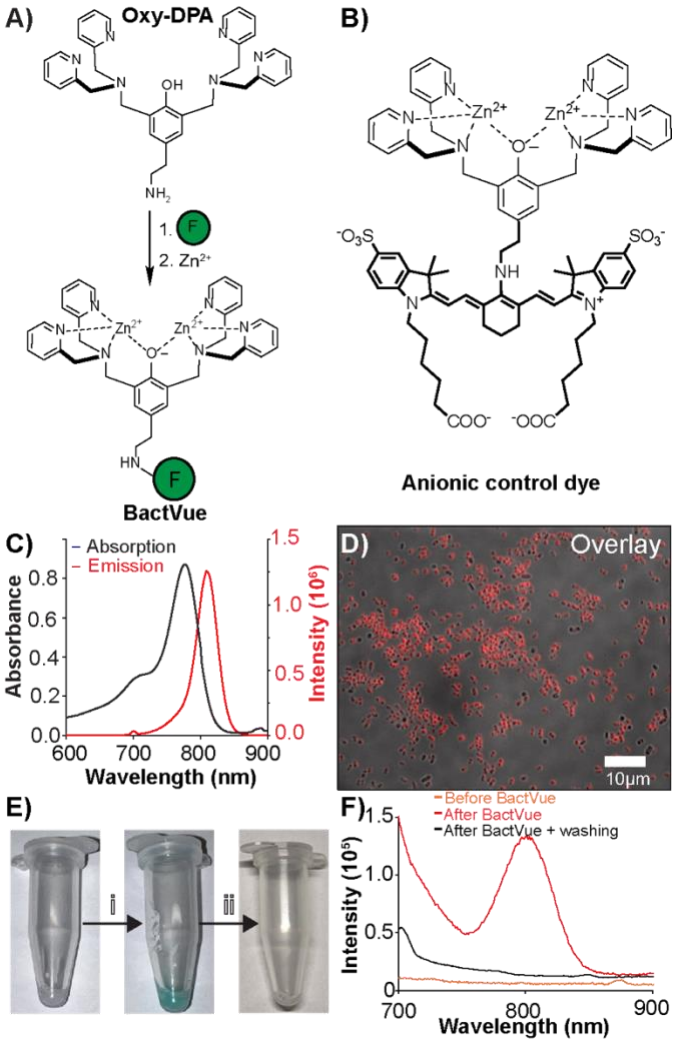

Figure 1. A) General synthesis of fluorescent probes. B) Structure of Anionic control dye. C) The absorption and emission spectra of BactVue in water (λ_{ex}=775 nm, λ_{em}=810 nm). D) Cy7 fluorescence image of UTI89 bacteria stained with BactVue overlayed with the bright-field image. E) Images of pelleted liposomes in Eppendorf tubes showing BactVue can reversibly associate with cell membranes. The leftmost image shows the pellet before treatment with BactVue, followed by (i) treatment with BactVue, which causes staining, but (ii) after washing, the dye is removed, causing the liposomes to return to their original color. F) Emission spectrum of before addition of BactVue (orange line) liposomes after incubation with BactVue (red line) and liposomes after washing (black line) showing that BactVue reversibly stains the liposomes.

BactVue was prepared straightforwardly by covalently connecting the Oxy-DPA ligand to the appropriate Cy7 fluorophore (F), followed by treatment with two molar equivalents of $Zn(NO_3)_2$

https://doi.org/10.26434/chemrxiv-2024-h3p4f **ORCID:** https://orcid.org/0000-0001-6400-8106 Content not peer-reviewed by ChemRxiv. **License:** CC BY-NC-ND 4.0

(**Figure 1A**). To demonstrate the importance of the charge-neutral characteristic of BactVue, we also prepared an Anionic control dye (**Figure 1B**). Both molecular probes were soluble in water. As expected for Cy7 dyes, BactVue exhibited an intense absorption peak at 775 nm with fluorescence emission at 810 nm (**Figure 1C**), and Anionic control dye exhibited very similar spectral properties (**Figure S1)**.

Initial experiments focused on *in vitro* staining of bacteria and involved the addition of BactVue (final concentration of 10 μM) to a culture of UTI89—a well-characterized laboratory strain of uropathogenic *E. coli*.[55, 56] After incubation, the stained bacterial cells were washed three times by repeating a sequence of centrifugation, removal of the aqueous solution, and pellet dispersion in fresh solution. The NIR fluorescence micrograph in **Figure 1D** reveals obvious and irreversible BactVue staining of the UTI89 bacteria. An identical staining procedure using Anionic control dye also produced staining of UTI89, as depicted in **Figure S2**. Additional fluorescence imaging evidence was gained by incubating separate UTI89(GFP) samples, a strain of UTI89 that expresses a stable form of green fluorescent protein, with BactVue or Anionic control dye. In both cases, there was high colocalization of the probe's Cy7 fluorescence with the green emission of the UTI89(GFP) bacteria (**Figure S3**).

The next round of experiments compared the capacity of BactVue and Anionic control dye to reversibly enter liposome bilayers that mimic the plasma membranes of mammalian cells. Unilamellar liposomes (~250 nm diameter) were prepared with phospholipids that mimic the composition of mammalian plasma membranes (*i.e.*, 98% w/w zwitterionic POPC and 2% w/w anionic DSPE-PEG2000). Separate samples of liposomes were incubated for 2 h with BactVue and Anionic control dye. After centrifugation and washing, the liposome pellets were examined, and clear differences in their capacity to interact with a lipid bilayer were observed. The liposomes treated with BactVue exhibited a green hue (**Figure S4**), and when the liposomes were resuspended in fresh buffer, fluorescence spectroscopy confirmed the presence of the BactVue

https://doi.org/10.26434/chemrxiv-2024-h3p4f **ORCID:** https://orcid.org/0000-0001-6400-8106 Content not peer-reviewed by ChemRxiv. **License:** CC BY-NC-ND 4.0

(**Figure 1F**). In contrast, the pellet of liposomes treated with Anionic control dye was not colored (**Figure S4**) and did not exhibit Cy7 fluorescence when resuspended. These results show that the charge-neutral yet water-soluble BactVue can favorably interact with a lipid bilayer while the charged dye does not. However, it is equally critical that the dye not become irreversibly trapped in the membrane, as this would prevent its ingress into the cytosol. To that end, we showed that the green color of BactVue-treated liposomes fades significantly after washing with pure buffer and leaves the membrane, returning to the supernatant with each wash. This contrasts with the bacterial staining experienced above, where the washing step did not dislodge the dye from the bacterial surface. This indicates that BactVue enters liposomes without permanently staining the membrane, gradually exiting during washing (**Figure S4**). These findings demonstrated that BactVue is a membrane-active molecular probe, suggesting it should permeate mammalian cell membranes and irreversibly bind to bacteria; thus, we moved to *in vitro* studies using cell culture.

The first set of *in vitro* imaging cell microscopy experiments examined human 5637 bladder carcinoma cells infected with UTI89(GFP), which enabled unambiguous visualization of the bacteria. The infected bladder cells were treated with gentamicin, an antibiotic that cannot penetrate the bladder cell plasma membrane and thus only kills the extracellular bacteria. Subsequently, the cells were washed repeatedly to ensure the complete removal of any extracellular bacteria and bacterial debris, and the collected supernatant fractions were cultured on CHROMagar plates, which showed no bacterial growth, thereby confirming the effectiveness of gentamicin to kill all extracellular bacteria. The infected bladder cells were sequentially incubated with BactVue for 2 h, washed, fixed, stained with the nuclear stain Hoechst, the cell plasma membrane stain, wheat germ agglutinin (WGA) rhodamine, and imaged using confocal laser scanning microscopy (CLSM). The representative micrographs in **Figure 2B** reflect the outcomes of three comparative experiments. In the first row, the human bladder cells were

https://doi.org/10.26434/chemrxiv-2024-h3p4f **ORCID:** https://orcid.org/0000-0001-6400-8106 Content not peer-reviewed by ChemRxiv. **License:** CC BY-NC-ND 4.0

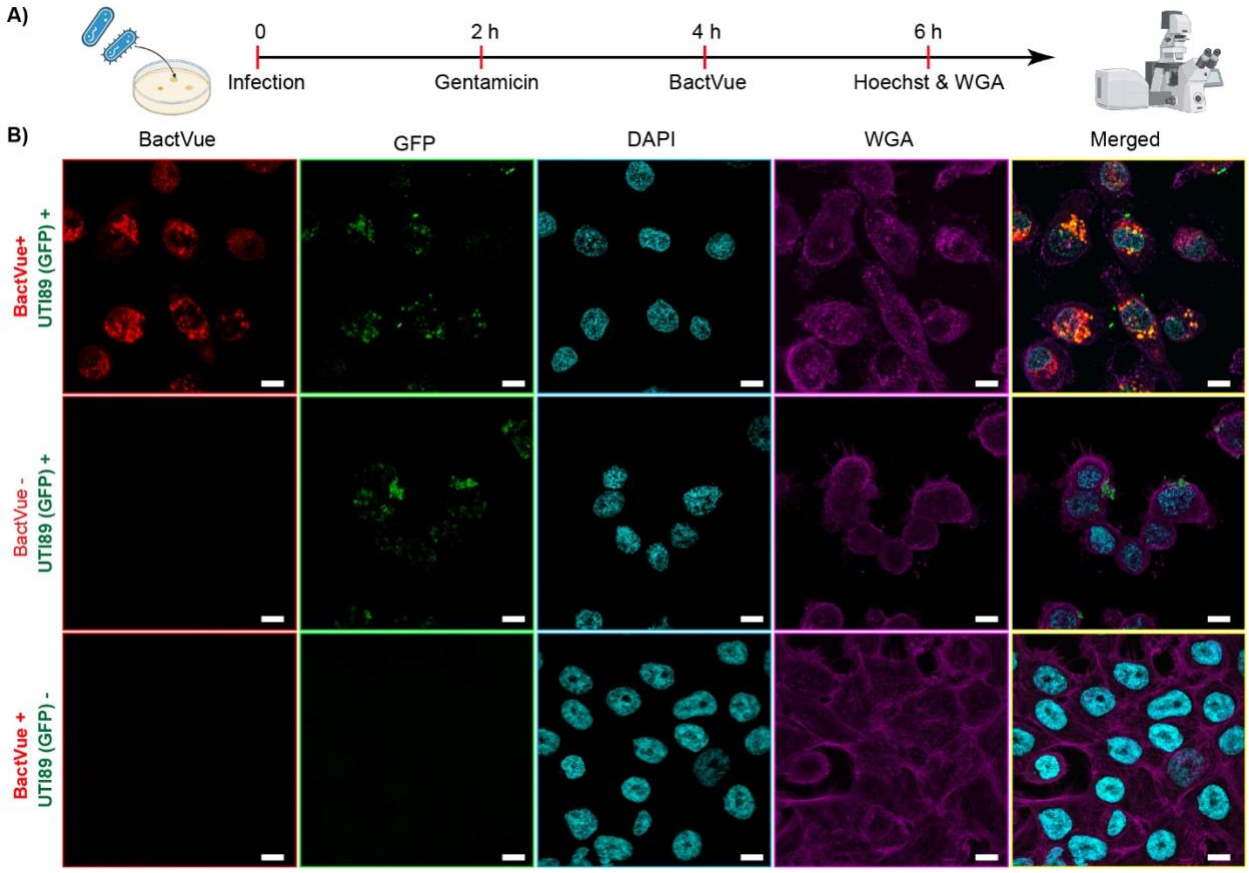

Figure 2: A) Schematic illustration of the experiment workflow for staining human 5637 bladder carcinoma cells infected with UTI89(GFP) bacteria. The 5637 bladder cells were infected with UTI89(GFP) (10 bacterial cells per human cell), treated with membrane-impermeable antibiotic gentamicin (100 µg/mL), washed, treated with BactVue (10 µM), washed, and fixed, treated with Hoechst/WGA rhodamine, washed, and then imaged on a confocal microscope. B) Confocal imaging: In the first row, cells were infected with UTI89(GFP), treated with gentamicin, and then BactVue was added. In the second row, cells were infected with UTI89(GFP) and treated with gentamicin, and BactVue was not added. In the third row, cells were not infected but treated with gentamicin and BactVue. Hoechst (λ_{ex}=350 nm, λ_{em}=461 nm), GFP (λ_{ex}=395 nm, λ_{em}=509 nm), WGA Rhodamine (λ_{ex}=570 nm, λ_{em}=590 nm) and Cy7 (λ_{ex}=730 nm, λ_{em}=779 nm). Scale bar =10 µm. Video in SI (Movie 1-5)

infected with UTI89(GFP), treated with gentamicin to kill extracellular bacteria, and then BactVue was added. In this case, intracellular staining of UTI89(GFP) by BactVue was indicated by a high Pearson colocalization coefficient of 0.72 for the GFP and Cy7 fluorescence. In the second row, bladder cells were infected with UTI89(GFP) and treated with the membrane-impermeable antibiotic gentamicin, but BactVue was not added, and there was no intracellular Cy7

https://doi.org/10.26434/chemrxiv-2024-h3p4f **ORCID:** https://orcid.org/0000-0001-6400-8106 Content not peer-reviewed by ChemRxiv. **License:** CC BY-NC-ND 4.0

fluorescence. Note that some bacteria appear extracellular, though they are enveloped in a cellular membrane—likely a phagocytic cup; thus, these bacteria are 'intracellular.' In the third row, cells were not infected with bacteria but treated with gentamicin and BactVue, and no intracellular Cy7 fluorescence was observed.

To rule out the possibility that our infection was somehow permeabilizing or destabilizing the membrane or that we were staining bacteria on the surface of cells that were then entering the cell, we conducted a control experiment using our Anionic control dye. A sample of human 5637 bladder cells infected with UTI89(GFP) was treated with gentamicin, followed by washing to eliminate all extracellular bacteria. The sample was split into two identical batches, and each batch was separately incubated with BactVue or membrane-impermeable Anionic control dye under the same conditions for 2 h. Following incubation, any extracellular fluorescent probe was removed through washing, and the bladder cells were lysed with 0.1% Triton X-100. The released intracellular bacteria were collected as a pellet after centrifugation, and fluorescence microscopy of the dispersed pellet revealed bacterial staining by BactVue but no bacterial staining by the Anionic control dye (**Figure S5**). These results show that BactVue penetrates the bladder cell membranes and stains the intracellular bacteria, while the Anionic control dye lacks this capability. In other words, the plasma membrane of the infected bladder cells is sufficiently intact that it prevents permeation of Anionic control dye, which has a polyanionic fluorophore; however, BactVue permeates the plasma membrane, which has the same Zn-Oxy-DPA targeting unit but a charge neutral fluorophore. Since the anionic control dye stains bacteria just as well as BactVue, it also shows that membrane-bound or "free" bacteria are not being stained and subsequently taken in by the cells. Taken together, these results show that BactVue uniquely can enter an intact cell membrane and selectively stain the bacteria already inside the cell.

https://doi.org/10.26434/chemrxiv-2024-h3p4f **ORCID:** https://orcid.org/0000-0001-6400-8106 Content not peer-reviewed by ChemRxiv. **License:** CC BY-NC-ND 4.0

Fluorescence imaging of UTI89 infection in living mouse bladder.

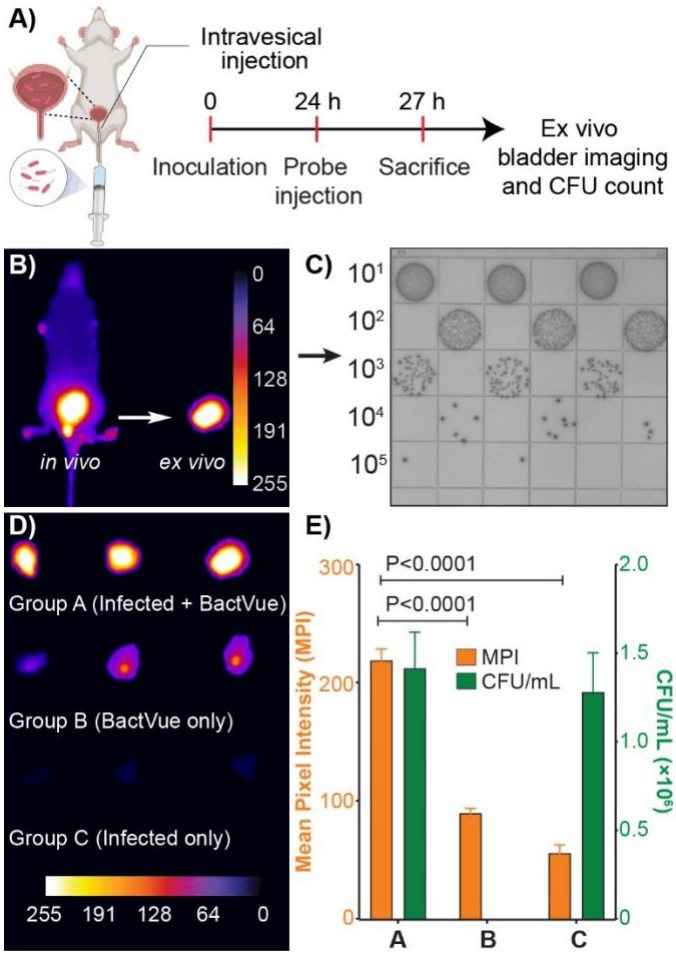

Figure 3. A) Schematic illustration of the experiment workflow. B) *In vivo* and *ex vivo* fluorescence images of a mouse bladder infected with UTI89 (50 µL of 1 ×10^7 CFU). C) Bacterial colonies grown from bladder homogenates (n=3) with different dilution factors. D) *Ex vivo* fluorescence images of three groups of mouse bladders (n=3 for each group) that had been dosed with UTI89 (50 µL of 1 ×10^7 CFU) or BactVue (50 µL of 50 µM). E) Quantification of fluorescence and bacteria burden in the three groups of mouse bladders in panel D as fluorescence mean pixel intensity (MPI) or CFU/mL, respectively (n=3 for each group). Statistical significance was determined by a One-way ANOVA.

The favorable *in vitro* microscopy results motivated us to pursue NIR fluorescence imaging of an *in vivo* model of UTI. The experimental goal was to determine if BactVue could differentiate between infected and non-infected cohorts. Our experimental approach is summarized in **Figure 3A**. Nine female BALB/c mice were divided into three groups; groups A and C received

https://doi.org/10.26434/chemrxiv-2024-h3p4f **ORCID:** https://orcid.org/0000-0001-6400-8106 Content not peer-reviewed by ChemRxiv. **License:** CC BY-NC-ND 4.0

intravesical (directly into the bladder) administration of UTI89 bacteria (50 µL of 1 ×10^7 CFU) via a catheter and were allowed to incubate for 24 h, while group B remained uninfected. Subsequently, groups A and B received intravesical doses of BactVue and all the living mice were imaged periodically over 3 h. It is worth mentioning that BactVue is sufficiently bright to visualize the infected bladder inside the intact animal and the *ex vivo* bladder (**Figure 3B**). After mouse sacrifice, the bladders were extracted for *ex vivo* fluorescence imaging. The bacterial count within each bladder was determined by homogenizing the bladder tissue, then by plating serially diluted aliquots of homogenate onto CHROMagar culture plates and quantifying the CFU/mL. The bacterial colony data in **Figure S6** confirms that each mouse bladder in group A contained essentially equal counts of UTI89 bacteria. *In vivo* fluorescence imaging of the mice in group B (the non-infected group injected with BactVue) revealed a large time-dependent decrease in bladder signal over the 3 h period, reflecting BactVue clearance from the bladder owing to urination (**Figure S7**). In contrast, *in vivo* fluorescence imaging of the mice in group A (infected mice injected with BactVue) exhibited a strong bladder signal that hardly changed over the 3 h period, indicating strong binding and retention of BactVue to the UTI89 bacteria in the bladder (**Figure S7**). Fluorescent images of the bladders extracted *ex vivo* confirmed the *in vivo* imaging trend, that is, strong retention of the Cy7 fluorescence signal in the bladders of group A mice (infected and treated with BactVue) and decreased fluorescence signal in the group B and C mice (**Figure 3D**). Statistical analysis (one-way ANOVA) of the *ex vivo* images confirmed a significant difference in fluorescence intensity between the infected (Group A) and non-infected (Group B) mice (**Figure 3E**). Though intravesical administration of BactVue would be a clinically useful way to identify intracellular bacteria, we further demonstrated that BactVue could target infected bladder tissue following tail vein injection. Mice injected with BactVue clearly excreted the dye via the urinary tract, where we observed significant fluorescence in the bladders of the infected mice, while the non-infected mice showed minimal fluorescence (**Figure S8**). Collectively, the *in vivo*

https://doi.org/10.26434/chemrxiv-2024-h3p4f **ORCID:** https://orcid.org/0000-0001-6400-8106 Content not peer-reviewed by ChemRxiv. **License:** CC BY-NC-ND 4.0

and *ex vivo* imaging results show that BactVue can identify infected bladders in a living mouse model of UTI.

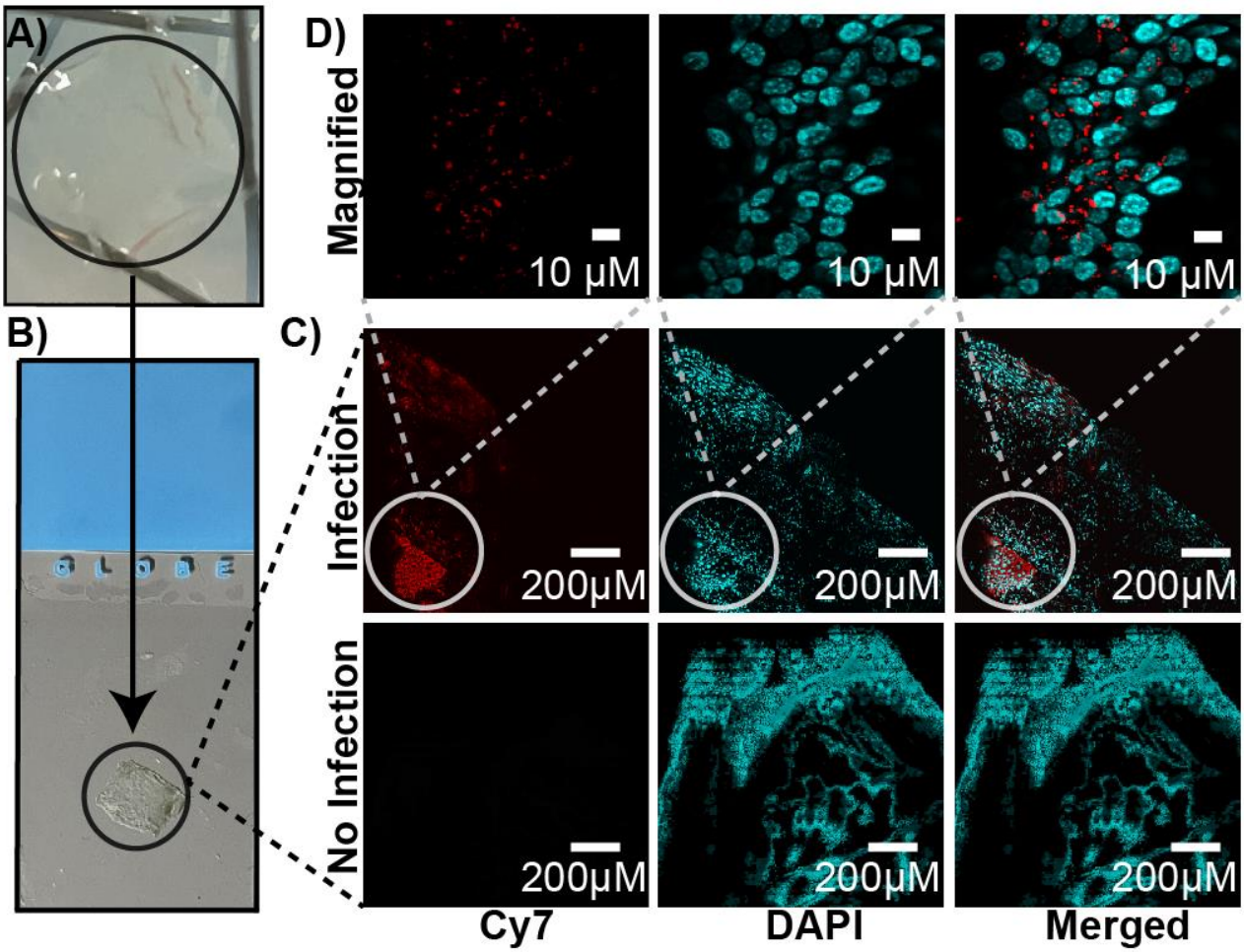

Figure 4: Images of extracted mouse bladders. Infected mice were given intravesical injections of UTI89 bacteria (50 μL of 1 ×10^7 CFU) and 24 hours later BactVue (50 μL of a 50 μM solution) was delivered via intravesical injection. A) Stretched mouse bladder lumen on agar bed. B) Mouse bladder stretched over a microscope slide C) Stitched CLSM images showing fluorescence reconstruction of an entire bladder section from an infected mouse and non-infected mouse, BactVue fluorescence colored red, and Hoechst nuclear fluorescence colored cyan. D) Magnified CLSM images of the infected mouse bladder in panel C). Video in SI (Movie 6 and 7).

Supporting fluorescence microscopy evidence that BactVue selectively targeted the intracellular UTI89 bacteria within infected bladder tissue was gathered by *ex vivo* analysis of the excised bladders using CLSM. An experiment compared two cohorts of female BALB/c mice—the non-

https://doi.org/10.26434/chemrxiv-2024-h3p4f **ORCID:** https://orcid.org/0000-0001-6400-8106 Content not peer-reviewed by ChemRxiv. **License:** CC BY-NC-ND 4.0

infected group versus the UTI89-infected group, each n=3. The infected group received an intravesical dose of UTI89 (50 µL of 1 ×10^7 CFU), whereas the non-infected group received an injection of 0.9% saline. After 24 h, both groups received intravesical injections of BactVue. The mice rested for 3 h and were allowed to drink water and urinate. The mice were sacrificed at that time, and the bladders were extracted. The bladders were longitudinally sectioned (**Figure 4A**), stretched with the luminal side facing upwards, fixed, and stained with the nuclear dye Hoechst. The sectioned bladders were imaged using CLSM with multiple fluorescence images stitched together to reconstruct a full-sized image. There was no Cy7 fluorescence signal in the bladders

from the non-infected group (**Figure 4C bottom**), indicating no retention of BactVue in the bladder tissue. In contrast, there was strong Cy7 fluorescence in localized areas of the bladders from the infected group (**Figure 4C top**), indicating retention of BactVue. This is an interesting result and aligns with clinical reports of patients with active cystitis that the infections are not diffuse, but seem to occur in localized areas of infection around the bladder.[57, 58] At higher magnification (**Figure 4D**), the BactVue fluorescence appeared as distinctive rod-like and punctate spots, and a stacked 3D reconstruction of the CLSM images revealed the spots were located within the bladder cells (see Movie 6 in SI). We conclude that BactVue selectively stains the intracellular UTI89 bacteria in the mouse bladder epithelial tissue.

Conclusion

BactVue is the first example of a new class of molecular probes that can target intracellular UPEC within infected bladder cells in cell culture and within a living mouse model of UTI. There is an opportunity to develop new diagnostic methods that use near-infrared fluorescent BactVue to visualize the location of infected bladder cells within an active UTI. It should be possible to synthetically alter the structure of the reporter group and create molecular probes for imaging UTI

https://doi.org/10.26434/chemrxiv-2024-h3p4f **ORCID:** https://orcid.org/0000-0001-6400-8106 Content not peer-reviewed by ChemRxiv. **License:** CC BY-NC-ND 4.0

using other modalities such as MRI or PET/SPECT.[32, 59] There is also potential to develop therapeutic approaches using the selective targeting ability of the Zn-Oxy-DPA unit.[29] Light-based therapies using appropriately modified versions of BactVue are particularly attractive since there are already effective clinical methods to illuminate the bladder with light.[60] Moreover, light-based therapies such as photodynamic therapy have the potential to eradicate drug-resistant UPEC, which is often a major factor in the etiology of recurring UTIs.[61, 62] We also envision new classes of antibiotic drug conjugates that exploit the selective targeting of intracellular UPEC by the Zn-Oxy-DPA unit. In this regard, it is worth noting that Zn-DPA conjugates of antibiotics and anticancer drugs have been reported and found to produce promising therapeutic effects.[63-65]

Conflicts of interest:

The authors declare that they have no competing interests.

Funding information:

We are grateful for funding from the NIH (R35GM136212 to B.S, 1R21AI169323-01 to N.J.D, and 1R21DK140688 to J.J.G. and N.J.D.) and the Welch Foundation (Grant no. AT-1989-20190330 to J.J.G).

Acknowledgements:

We thank Jon Chiaramonte for synthesizing a batch of BactVue and the University of Texas at Dallas Lab Animal Resource Center (LARC) for their assistance in animal care.

Author contributions:

Conceptualization: J. J. G., N. J. D, B. D. S Methodology: S. Koirala, Y. H. W., J. G., S. C., Investigation: S. Koirala, Y. H. W., D. H. L, J. G., R. N. E., S. C., M. A. G., T. Q. N. N., O. T., I. T., S. Kumari, L. M. H., T. S. H., Manuscript preparation: S. Koirala, J.G., B. D. S, N. J. D. and J. J. G. Funding acquisition: J. J. G, N. J. D., and B. D. S.

https://doi.org/10.26434/chemrxiv-2024-h3p4f **ORCID:** https://orcid.org/0000-0001-6400-8106 Content not peer-reviewed by ChemRxiv. **License:** CC BY-NC-ND 4.0

References

(1) Foxman, B. The epidemiology of urinary tract infection. *Nat Rev Urol* **2010**, *7* (12), 653-660. DOI: 10.1038/nrurol.2010.190 From NLM Medline.

(2) Medina, M.; Castillo-Pino, E. An introduction to the epidemiology and burden of urinary tract infections. *Ther Adv Urol* **2019**, *11*, 1756287219832172. DOI: 10.1177/1756287219832172 From NLM PubMed-not-MEDLINE.

(3) Al-Badr, A.; Al-Shaikh, G. Recurrent Urinary Tract Infections Management in Women: A review. *Sultan Qaboos Univ Med J* **2013**, *13* (3), 359-367. DOI: 10.12816/0003256 From NLM PubMed-not-MEDLINE.

(4) Flores-Mireles, A. L.; Walker, J. N.; Caparon, M.; Hultgren, S. J. Urinary tract infections: epidemiology, mechanisms of infection and treatment options. *Nat Rev Microbiol* **2015**, *13* (5), 269-284. DOI: 10.1038/nrmicro3432 From NLM Medline.

(5) Luzuriaga, M. A.; Herbert, F. C.; Brohlin, O. R.; Gadhvi, J.; Howlett, T.; Shahrivarkevishahi, A.; Wijesundara, Y. H.; Venkitapathi, S.; Veera, K.; Ehrman, R.; et al. Metal-Organic Framework Encapsulated Whole-Cell Vaccines Enhance Humoral Immunity against Bacterial Infection. *ACS Nano* **2021**, *15* (11), 17426-17438. DOI: 10.1021/acsnano.1c03092 From NLM Medline.

(6) Totsika, M.; Moriel, D. G.; Idris, A.; Rogers, B. A.; Wurpel, D. J.; Phan, M. D.; Paterson, D. L.; Schembri, M. A. Uropathogenic Escherichia coli mediated urinary tract infection. *Curr Drug Targets* **2012**, *13* (11), 1386-1399. DOI: 10.2174/138945012803530206 From NLM Medline.

(7) Shah, C.; Baral, R.; Bartaula, B.; Shrestha, L. B. Virulence factors of uropathogenic Escherichia coli (UPEC) and correlation with antimicrobial resistance. *BMC Microbiol* **2019**, *19* (1), 204. DOI: 10.1186/s12866-019-1587-3 From NLM Medline.

(8) Liu, Y.; Jia, Y.; Yang, K.; Wang, Z. Heterogeneous Strategies to Eliminate Intracellular Bacterial Pathogens. *Front Microbiol* **2020**, *11*, 563. DOI: 10.3389/fmicb.2020.00563 From NLM PubMed-not-MEDLINE.

(9) Hannan, T. J.; Totsika, M.; Mansfield, K. J.; Moore, K. H.; Schembri, M. A.; Hultgren, S. J. Host-pathogen checkpoints and population bottlenecks in persistent and intracellular uropathogenic Escherichia coli bladder infection. *FEMS Microbiol Rev* **2012**, *36* (3), 616-648. DOI: 10.1111/j.1574-6976.2012.00339.x From NLM Medline.

(10) Venkitapathi, S.; Wijesundara, Y. H.; Cornelius, S. A.; Herbert, F. C.; Gassensmith, J. J.; Zimmern, P. E.; De Nisco, N. J. Conserved FimK Truncation Coincides with Increased Expression of Type 3 Fimbriae and Cultured Bladder Epithelial Cell Association in Klebsiella quasipneumoniae. *J Bacteriol* **2022**, *204* (9), e0017222. DOI: 10.1128/jb.00172-22 From NLM Medline.

(11) Anderson, G. G.; Dodson, K. W.; Hooton, T. M.; Hultgren, S. J. Intracellular bacterial communities of uropathogenic Escherichia coli in urinary tract pathogenesis. *Trends Microbiol* **2004**, *12* (9), 424-430. DOI: 10.1016/j.tim.2004.07.005 From NLM Medline.

(12) De Nisco, N. J.; Neugent, M.; Mull, J.; Chen, L.; Kuprasertkul, A.; de Souza Santos, M.; Palmer, K. L.; Zimmern, P.; Orth, K. Direct Detection of Tissue-Resident Bacteria and Chronic Inflammation in the Bladder Wall of Postmenopausal Women with Recurrent Urinary

https://doi.org/10.26434/chemrxiv-2024-h3p4f **ORCID:** https://orcid.org/0000-0001-6400-8106 Content not peer-reviewed by ChemRxiv. **License:** CC BY-NC-ND 4.0

Tract Infection. *J Mol Biol* **2019**, *431* (21), 4368-4379. DOI: 10.1016/j.jmb.2019.04.008 From NLM Medline.

(13) Bower, J. M.; Eto, D. S.; Mulvey, M. A. Covert operations of uropathogenic Escherichia coli within the urinary tract. *Traffic* **2005**, *6* (1), 18-31.

(14) Ulett, G. C.; Totsika, M.; Schaale, K.; Carey, A. J.; Sweet, M. J.; Schembri, M. A. Uropathogenic Escherichia coli virulence and innate immune responses during urinary tract infection. *Curr Opin Microbiol* **2013**, *16* (1), 100-107. DOI: 10.1016/j.mib.2013.01.005 From NLM Medline.

(15) Xu, R.; Deebel, N.; Casals, R.; Dutta, R.; Mirzazadeh, M. A New Gold Rush: A Review of Current and Developing Diagnostic Tools for Urinary Tract Infections. *Diagnostics (Basel)* **2021**, *11* (3), 479. DOI: 10.3390/diagnostics11030479 From NLM PubMed-not-MEDLINE.

(16) Masajtis-Zagajewska, A.; Nowicki, M. New markers of urinary tract infection. *Clin Chim Acta* **2017**, *471*, 286-291. DOI: 10.1016/j.cca.2017.06.003 From NLM Medline.

(17) Chu, C. M.; Lowder, J. L. Diagnosis and treatment of urinary tract infections across age groups. *Am J Obstet Gynecol* **2018**, *219* (1), 40-51. DOI: 10.1016/j.ajog.2017.12.231 From NLM Medline.

(18) Schmiemann, G.; Kniehl, E.; Gebhardt, K.; Matejczyk, M. M.; Hummers-Pradier, E. The diagnosis of urinary tract infection: a systematic review. *Dtsch Arztebl Int* **2010**, *107* (21), 361-367. DOI: 10.3238/arztebl.2010.0361 From NLM Medline.

(19) Najeeb, S.; Munir, T.; Rehman, S.; Hafiz, A.; Gilani, M.; Latif, M. Comparison of urine dipstick test with conventional urine culture in diagnosis of urinary tract infection. *J Coll Physicians Surg Pak* **2015**, *25* (2), 108-110. From NLM Medline.

(20) Dadzie, I.; Quansah, E.; Puopelle Dakorah, M.; Abiade, V.; Takyi-Amuah, E.; Adusei, R. The Effectiveness of Dipstick for the Detection of Urinary Tract Infection. *Can J Infect Dis Med Microbiol* **2019**, *2019*, 8642628. DOI: 10.1155/2019/8642628 From NLM PubMed-not-MEDLINE.

(21) Fritzenwanker, M.; Imirzalioglu, C.; Chakraborty, T.; Wagenlehner, F. M. Modern diagnostic methods for urinary tract infections. *Expert Rev Anti Infect Ther* **2016**, *14* (11), 1047-1063. DOI: 10.1080/14787210.2016.1236685 From NLM Medline.

(22) Berry, R. E.; Klumpp, D. J.; Schaeffer, A. J. Urothelial cultures support intracellular bacterial community formation by uropathogenic Escherichia coli. *Infect Immun* **2009**, *77* (7), 2762-2772. DOI: 10.1128/IAI.00323-09 From NLM Medline.

(23) Scott, V. C.; Haake, D. A.; Churchill, B. M.; Justice, S. S.; Kim, J. H. Intracellular Bacterial Communities: A Potential Etiology for Chronic Lower Urinary Tract Symptoms. *Urology* **2015**, *86* (3), 425-431. DOI: 10.1016/j.urology.2015.04.002 From NLM Medline.

(24) Anderson, G. G.; Martin, S. M.; Hultgren, S. J. Host subversion by formation of intracellular bacterial communities in the urinary tract. *Microbes Infect* **2004**, *6* (12), 1094-1101. DOI: 10.1016/j.micinf.2004.05.023 From NLM Medline.

(25) Lehar, S. M.; Pillow, T.; Xu, M.; Staben, L.; Kajihara, K. K.; Vandlen, R.; DePalatis, L.; Raab, H.; Hazenbos, W. L.; Morisaki, J. H.; et al. Novel antibody-antibiotic conjugate eliminates intracellular S. aureus. *Nature* **2015**, *527* (7578), 323-328. DOI: 10.1038/nature16057 From NLM Medline.

https://doi.org/10.26434/chemrxiv-2024-h3p4f **ORCID:** https://orcid.org/0000-0001-6400-8106 Content not peer-reviewed by ChemRxiv. **License:** CC BY-NC-ND 4.0

(26) Jiang, Y.; Han, M.; Bo, Y.; Feng, Y.; Li, W.; Wu, J. R.; Song, Z.; Zhao, Z.; Tan, Z.; Chen, Y.; et al. "Metaphilic" Cell-Penetrating Polypeptide-Vancomycin Conjugate Efficiently Eradicates Intracellular Bacteria via a Dual Mechanism. *ACS Cent Sci* **2020**, *6* (12), 2267-2276. DOI: 10.1021/acscentsci.0c00893 From NLM PubMed-not-MEDLINE.

(27) Kuroki, A.; Kengmo Tchoupa, A.; Hartlieb, M.; Peltier, R.; Locock, K. E. S.; Unnikrishnan, M.; Perrier, S. Targeting intracellular, multi-drug resistant Staphylococcus aureus with guanidinium polymers by elucidating the structure-activity relationship. *Biomaterials* **2019**, *217*, 119249. DOI: 10.1016/j.biomaterials.2019.119249 From NLM Medline.

(28) Lei, E. K.; Pereira, M. P.; Kelley, S. O. Tuning the intracellular bacterial targeting of peptidic vectors. *Angew Chem Int Ed Engl* **2013**, *52* (37), 9660-9663. DOI: 10.1002/anie.201302265 From NLM Medline.

(29) Rice, D. R.; Clear, K. J.; Smith, B. D. Imaging and therapeutic applications of zinc(ii)-dipicolylamine molecular probes for anionic biomembranes. *Chem Commun (Camb)* **2016**, *52* (57), 8787-8801. DOI: 10.1039/c6cc03669d From NLM Medline.

(30) Li, P.; Zhou, C.; Rayatpisheh, S.; Ye, K.; Poon, Y. F.; Hammond, P. T.; Duan, H.; Chan-Park, M. B. Cationic peptidopolysaccharides show excellent broad-spectrum antimicrobial activities and high selectivity. *Advanced Materials* **2012**, *24* (30), 4130-4137.

(31) Hanshaw, R. G.; Hilkert, S. M.; Jiang, H.; Smith, B. D. An indicator displacement system for fluorescent detection of phosphate oxyanions under physiological conditions. *Tetrahedron letters* **2004**, *45* (47), 8721-8724.

(32) Aweda, T. A.; Muftuler, Z. F. B.; Massicano, A. V. F.; Gadhia, D.; McCarthy, K. A.; Queern, S.; Bandyopadhyay, A.; Gao, J.; Lapi, S. E. Radiolabeled Cationic Peptides for Targeted Imaging of Infection. *Contrast Media Mol Imaging* **2019**, *2019*, 3149249. DOI: 10.1155/2019/3149249 From NLM Medline.

(33) Ji, Y.; Li, G.; Wang, J.; Piao, C.; Zhou, X. Recent Progress in Identifying Bacteria with Fluorescent Probes. *Molecules* **2022**, *27* (19), 6440. DOI: 10.3390/molecules27196440 From NLM Medline.

(34) Jiou, J.; Chiravuri, K.; Gudapati, A.; J Gassensmith, J. The Chemistry of Confined Spaces. *Current Organic Chemistry* **2014**, *18* (15), 2002-2009.

(35) Biniecki, S.; Kabzinska, S. Synthesis of bis-(pyridylmethyl)-amines. In *Annales pharmaceutiques francaises*, 1964; Vol. 22, pp 685-687.

(36) Ngo, H. T.; Liu, X.; Jolliffe, K. A. Anion recognition and sensing with Zn(II)-dipicolylamine complexes. *Chem Soc Rev* **2012**, *41* (14), 4928-4965. DOI: 10.1039/c2cs35087d From NLM Medline.

(37) Clear, K. J.; Harmatys, K. M.; Rice, D. R.; Wolter, W. R.; Suckow, M. A.; Wang, Y.; Rusckowski, M.; Smith, B. D. Phenoxide-Bridged Zinc(II)-Bis(dipicolylamine) Probes for Molecular Imaging of Cell Death. *Bioconjug Chem* **2016**, *27* (2), 363-375. DOI: 10.1021/acs.bioconjchem.5b00447 From NLM Medline.

(38) DiVittorio, K. M.; Leevy, W. M.; O'Neil, E. J.; Johnson, J. R.; Vakulenko, S.; Morris, J. D.; Rosek, K. D.; Serazin, N.; Hilkert, S.; Hurley, S. Zinc (II) coordination complexes as membrane-active fluorescent probes and antibiotics. *ChemBioChem* **2008**, *9* (2), 286-293.

https://doi.org/10.26434/chemrxiv-2024-h3p4f **ORCID:** https://orcid.org/0000-0001-6400-8106 Content not peer-reviewed by ChemRxiv. **License:** CC BY-NC-ND 4.0

(39) Jiang, H.; O'Neil E, J.; Divittorio, K. M.; Smith, B. D. Anion-mediated phase transfer of Zinc(II)-coordinated tyrosine derivatives. *Org Lett* **2005**, *7* (14), 3013-3016. DOI: 10.1021/ol0510421 From NLM Medline.

(40) Savastano, M.; Fiaschi, M.; Ferraro, G.; Gratteri, P.; Mariani, P.; Bianchi, A.; Bazzicalupi, C. Sensing Zn(2+) in Aqueous Solution with a Fluorescent Scorpiand Macrocyclic Ligand Decorated with an Anthracene Bearing Tail. *Molecules* **2020**, *25* (6), 1355. DOI: 10.3390/molecules25061355 From NLM Medline.

(41) Ruedas-Rama, M. J.; Hall, E. A. Azamacrocycle activated quantum dot for zinc ion detection. *Anal Chem* **2008**, *80* (21), 8260-8268. DOI: 10.1021/ac801396y From NLM Medline.

(42) Ahmad, T.; Waheed, A.; Abdel-Azeim, S.; Khan, S.; Ullah, N. Three new turn-on fluorescent sensors for the selective detection of Zn2+: Synthesis, properties and DFT studies. *Arabian Journal of Chemistry* **2022**, *15* (8), 104002.

(43) Dash, N.; Malakar, A.; Kumar, M.; Mandal, B. B.; Krishnamoorthy, G. Metal ion dependent “ON” intramolecular charge transfer (ICT) and “OFF” normal switching of the fluorescence: sensing of Zn2+ by ICT emission in living cells. *Sensors and Actuators B: Chemical* **2014**, *202*, 1154-1163.

(44) Usama, S. M.; Marker, S. C.; Hernandez Vargas, S.; AghaAmiri, S.; Ghosh, S. C.; Ikoma, N.; Tran Cao, H. S.; Schnermann, M. J.; Azhdarinia, A. Targeted Dual-Modal PET/SPECT-NIR Imaging: From Building Blocks and Construction Strategies to Applications. *Cancers (Basel)* **2022**, *14* (7), 1619. DOI: 10.3390/cancers14071619 From NLM PubMed-not-MEDLINE.

(45) Welsher, K.; Sherlock, S. P.; Dai, H. Deep-tissue anatomical imaging of mice using carbon nanotube fluorophores in the second near-infrared window. *Proc Natl Acad Sci U S A* **2011**, *108* (22), 8943-8948. DOI: 10.1073/pnas.1014501108 From NLM Medline.

(46) Demos, S. G.; Gandour-Edwards, R.; Ramsamooj, R.; White, R. Near-infrared autofluorescence imaging for detection of cancer. *J Biomed Opt* **2004**, *9* (3), 587-592. DOI: 10.1117/1.1688812 From NLM Medline.

(47) Paras, C.; Keller, M.; White, L.; Phay, J.; Mahadevan-Jansen, A. Near-infrared autofluorescence for the detection of parathyroid glands. *J Biomed Opt* **2011**, *16* (6), 067012. DOI: 10.1117/1.3583571 From NLM Medline.

(48) Li, D. H.; Gamage, R. S.; Oliver, A. G.; Patel, N. L.; Muhammad Usama, S.; Kalen, J. D.; Schnermann, M. J.; Smith, B. D. Doubly Strapped Zwitterionic NIR-I and NIR-II Heptamethine Cyanine Dyes for Bioconjugation and Fluorescence Imaging. *Angew Chem Int Ed Engl* **2023**, *62* (28), e202305062. DOI: 10.1002/anie.202305062 From NLM Medline.

(49) Shahrivarkevishahi, A.; Luzuriaga, M. A.; Herbert, F. C.; Tumac, A. C.; Brohlin, O. R.; Wijesundara, Y. H.; Adlooru, A. V.; Benjamin, C.; Lee, H.; Parsamian, P.; et al. PhotothermalPhage: A Virus-Based Photothermal Therapeutic Agent. *J Am Chem Soc* **2021**, *143* (40), 16428-16438. DOI: 10.1021/jacs.1c05090 From NLM Medline.

(50) Li, D. H.; Gamage, R. S.; Smith, B. D. Sterically Shielded Hydrophilic Analogs of Indocyanine Green. *J Org Chem* **2022**, *87* (17), 11593-11601. DOI: 10.1021/acs.joc.2c01229 From NLM Medline.

https://doi.org/10.26434/chemrxiv-2024-h3p4f **ORCID:** https://orcid.org/0000-0001-6400-8106 Content not peer-reviewed by ChemRxiv. **License:** CC BY-NC-ND 4.0

(51) Yang, N. J.; Hinner, M. J. Getting across the cell membrane: an overview for small molecules, peptides, and proteins. *Methods Mol Biol* **2015**, *1266*, 29-53. DOI: 10.1007/978-1-4939-2272-7_3 From NLM Medline.

(52) O'Neil, E. J.; Smith, B. D. Anion recognition using dimetallic coordination complexes. *Coordination Chemistry Reviews* **2006**, *250* (23-24), 3068-3080.

(53) Li, D. H.; Schreiber, C. L.; Smith, B. D. Sterically Shielded Heptamethine Cyanine Dyes for Bioconjugation and High Performance Near-Infrared Fluorescence Imaging. *Angew Chem Int Ed Engl* **2020**, *59* (29), 12154-12161. DOI: 10.1002/anie.202004449 From NLM Medline.

(54) Li, D. Structural Optimization of Heptamethine Cyanine Dyes; University of Notre Dame, 2022.

(55) Kulkarni, R.; Dhakal, B. K.; Slechta, E. S.; Kurtz, Z.; Mulvey, M. A.; Thanassi, D. G. Roles of putative type II secretion and type IV pilus systems in the virulence of uropathogenic Escherichia coli. *PLoS One* **2009**, *4* (3), e4752. DOI: 10.1371/journal.pone.0004752 From NLM Medline.

(56) Wright, K. J.; Seed, P. C.; Hultgren, S. J. Development of intracellular bacterial communities of uropathogenic Escherichia coli depends on type 1 pili. *Cell Microbiol* **2007**, *9* (9), 2230-2241. DOI: 10.1111/j.1462-5822.2007.00952.x From NLM Medline.

(57) Vazquez, J. A.; Sobel, J. D. Candidiasis. In *Essentials of clinical mycology*, Springer, 2010; pp 167-206.

(58) Hanno, P. M. Interstitial cystitis and related disorders. *Campbell's urology* **2002**, *1*, 631-670.

(59) Lee, H.; Shahrivarkevishahi, A.; Lumata, J. L.; Luzuriaga, M. A.; Hagge, L. M.; Benjamin, C. E.; Brohlin, O. R.; Parish, C. R.; Firouzi, H. R.; Nielsen, S. O.; et al. Supramolecular and biomacromolecular enhancement of metal-free magnetic resonance imaging contrast agents. *Chem Sci* **2020**, *11* (8), 2045-2050. DOI: 10.1039/c9sc05510j From NLM PubMed-not-MEDLINE.

(60) Evelyne, C. C.; de La Rosette, J. J.; de Reijke, T. M. Emerging optical techniques in advanced cystoscopy for bladder cancer diagnosis: A review of the current literature. *Indian Journal of Urology* **2011**, *27* (2), 245-251.

(61) Huang, Y. Y.; Wintner, A.; Seed, P. C.; Brauns, T.; Gelfand, J. A.; Hamblin, M. R. Antimicrobial photodynamic therapy mediated by methylene blue and potassium iodide to treat urinary tract infection in a female rat model. *Sci Rep* **2018**, *8* (1), 7257. DOI: 10.1038/s41598-018-25365-0 From NLM Medline.

(62) Tichaczek-Goska, D.; Glensk, M.; Wojnicz, D. The Enhancement of the Photodynamic Therapy and Ciprofloxacin Activity against Uropathogenic Escherichia coli Strains by Polypodium vulgare Rhizome Aqueous Extract. *Pathogens* **2021**, *10* (12), 1544. DOI: 10.3390/pathogens10121544 From NLM PubMed-not-MEDLINE.

(63) Yarlagadda, V.; Sarkar, P.; Samaddar, S.; Manjunath, G. B.; Mitra, S. D.; Paramanandham, K.; Shome, B. R.; Haldar, J. Vancomycin Analogue Restores Meropenem Activity against NDM-1 Gram-Negative Pathogens. *ACS Infect Dis* **2018**, *4* (7), 1093-1101. DOI: 10.1021/acsinfecdis.8b00011 From NLM Medline.

https://doi.org/10.26434/chemrxiv-2024-h3p4f **ORCID:** https://orcid.org/0000-0001-6400-8106 Content not peer-reviewed by ChemRxiv. **License:** CC BY-NC-ND 4.0

(64) Guan, D.; Chen, F.; Faridoon; Liu, J.; Li, J.; Lan, L.; Huang, W. Design and Synthesis of Pyrophosphate-Targeting Vancomycin Derivatives for Combating Vancomycin-Resistant Enterococci. *ChemMedChem* **2018**, *13* (16), 1644-1657. DOI: 10.1002/cmdc.201800252 From NLM Medline.

(65) Liu, Y. W.; Chen, Y. Y.; Hsu, C. Y.; Chiu, T. Y.; Liu, K. L.; Lo, C. F.; Fang, M. Y.; Huang, Y. C.; Yeh, T. K.; Pak, K. Y.; et al. Linker Optimization and Therapeutic Evaluation of Phosphatidylserine-Targeting Zinc Dipicolylamine-based Drug Conjugates. *J Med Chem* **2019**, *62* (13), 6047-6062. DOI: 10.1021/acs.jmedchem.9b00173 From NLM Medline.

https://doi.org/10.26434/chemrxiv-2024-h3p4f **ORCID:** https://orcid.org/0000-0001-6400-8106 Content not peer-reviewed by ChemRxiv. **License:** CC BY-NC-ND 4.0